Origins of the 1988 North American Drought

KEVIN E. TRENBERTH, GRANT W. BRANSTATOR, PHILLIP A. ARKIN

The 1988 summer drought in the United States was the most extensive in many years. Because the drought developed in different places at different times, not all regional effects can be traced to the same cause. Along the West Coast and in the northwestern United States drought conditions developed during 1987 in association with the 1986 to 1987 El Niño in the tropical Pacific Ocean. Record low rainfalls from April to June 1988 led to rapid development of drought in the North Central United States. Strong anticyclonic conditions and a northward displaced jet stream in the upper atmosphere over North America throughout this period were only part of a pronounced and distinctive wavetrain of anomalies in the atmospheric circulation that appeared to emanate from the tropical Pacific. Below average sea surface temperatures along the equator in the Pacific in the northern spring of 1988, combined with warmer than normal water from 10° to 20°N, led to a northward displaced but still active intertropical convergence zone (ITCZ) southeast of Hawaii. Results from a steady-state planetary-wave atmospheric model indicate that the atmospheric heating anomalies associated with the displaced ITCZ can force an anomalous wavetrain across North America similar to that observed. Land surface processes probably contributed to the severity and persistence of the drought; however, the large-scale atmospheric circulation perturbations associated with natural variations in the coupled atmosphere-ocean system in the tropical Pacific were most likely the primary cause.

WHAT WAS THE CAUSE OF THE 1988 SUMMER NORTH American drought? A common answer from meteorologists has been that the jet stream was displaced northward of its usual position so that storms, which tend to track along the path of the jet stream, were similarly displaced northward. As a result, rain-producing weather systems over the United States were weak and far between. Such an answer is, however, just a brief description of the weather patterns associated with the drought but does not get at the cause. A more satisfying response would address why the jet stream was displaced northward. In this article we investigate the origins of the drought by considering how it developed and the physical processes involved.

One physical phenomenon that has been linked to the drought is the greenhouse effect, which is the expected atmospheric warming resulting from the buildup in greenhouse gases, such as carbon dioxide, methane, and the chlorofluorocarbons (CFCs), all of which have increasing concentrations in the atmosphere because of man's activities (*1*). However, the greenhouse effect is gradual. Little difference in the radiative effects of greenhouse gases is expected between this year and last, but differences between this year and, say, 20 years ago should be noticeable. Climate simulations (*2*) indicate that a doubling of carbon dioxide concentrations could increase the frequency of summer droughts over North America. Thus, the greenhouse effect may tilt the balance such that conditions for droughts and heat waves are more likely, but it cannot be blamed for an individual drought.

Droughts are a naturally occurring phenomenon (*3–5*). There is usually a pocket of drought at least somewhere in the United States at any given time. The most extensive extreme and severe droughts in the past have occurred in the 1930s (the dust bowl era) and the 1950s (*6*), apparently as a part of natural variations in the climate system. We examine the 1988 drought in this context of natural interannual variability.

The 1988 drought developed at different times in different parts of the country, and not all of these regional events can be traced to the same cause. Oceanic conditions associated with the 1987 El Niño may have been a primary factor in setting up the drought conditions that occurred during that year in West Coast and Northern Great Plains regions. We focus on the relatively rapid development of the Midwest United States drought in April to June 1988, and examine, using results from an atmospheric planetary-wave model, how it may have been linked to the very different distribution of sea surface temperatures in the tropical Pacific Ocean that occurred as an aftermath of the 1987 El Niño.

The 1986–1987 El Niño, Prelude to the Drought

The development of the 1988 drought is illustrated by the Palmer drought index (7) (Fig. 1). In October 1986, soil moisture content was above average in much of the nation except for the Southeast. By April 1987 (not shown), the dry conditions in the Southeast had ameliorated to a large extent but the development of the drought on the West Coast and northwestern United States was well under way. By April 1988 (second panel of Fig. 1), drought conditions had become pervasive along the West Coast and northern United States (extending from Idaho to Minnesota) and dry conditions had returned to parts of the Southeast.

In addition to being a year of West Coast drought, 1987 was also a time when El Niño conditions occurred in the tropical Pacific Ocean (*8, 9*) (Fig. 2). During an El Niño event, sea surface temperatures (SSTs) are above normal along the equator from South America to the central Pacific. These events are also associated with large displacements of the major rain-producing convergence zones in the tropics and atmospheric circulation changes such as the

K. E. Trenberth and G. W. Branstator are scientists at the National Center for Atmospheric Research, Boulder, CO 80307. P. A. Arkin is a scientist at the Climate Analysis Center, National Meteorological Center, National Oceanic and Atmospheric Administration, Camp Springs, MD 20233.

Southern Oscillation. During northern winter months, such conditions generally favor the development of a stronger than normal ridge of high pressure near the west coast of the United States and lower pressures in the Aleutian Low over the north Pacific Ocean (*10*). These patterns are referred to as teleconnections. The redistribution of latent heating associated with the disruption in normal tropical convection patterns sets up these teleconnections by forcing anomalous Rossby waves in the upper troposphere that propagate into midlatitudes and interact with the climatological stationary mean waves in the Northern Hemisphere circulation (*11, 12*).

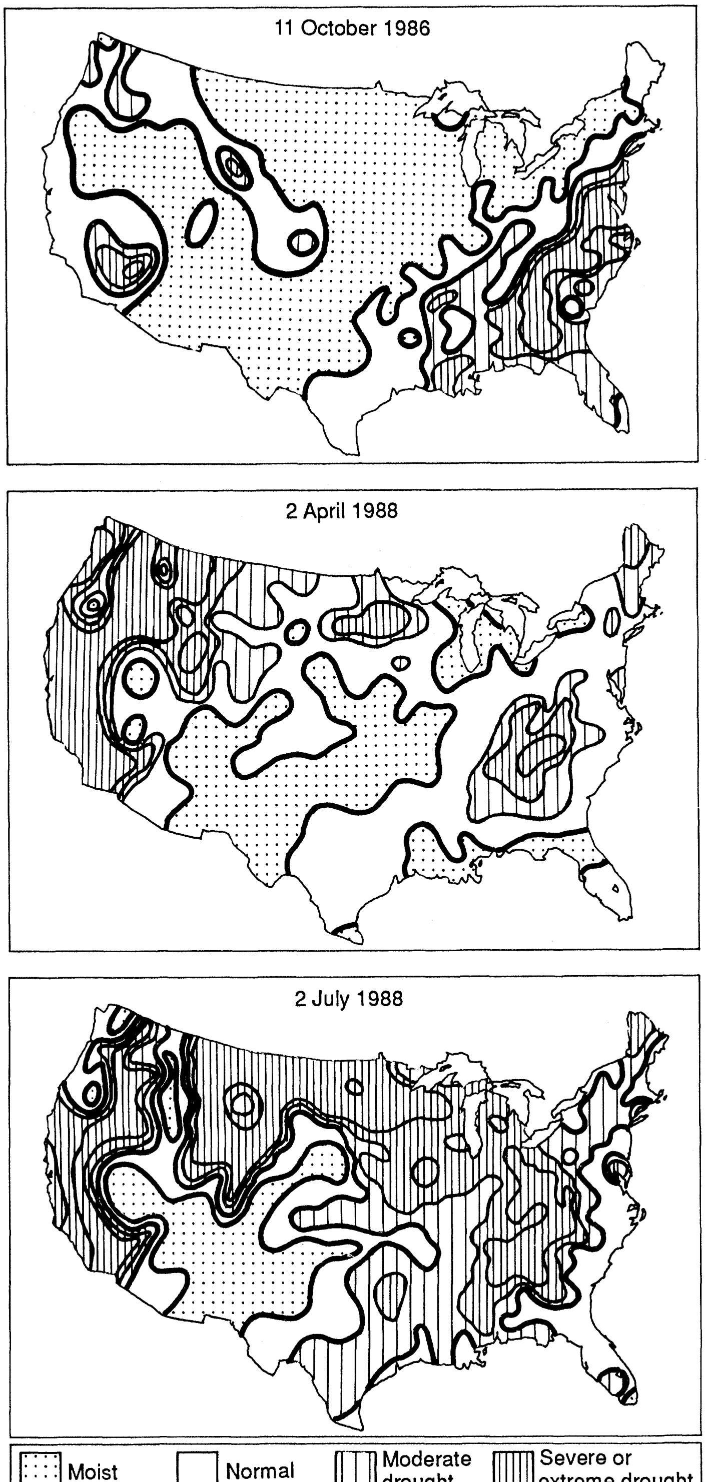

Fig. 1. Maps of the Palmer drought index (*7*) over the United States for the dates indicated. Categories ranging from moist (stippled), normal (no pattern), moderate drought (sparse hatching), severe drought (dense hatching), and extreme drought (dense hatching, innermost contour) are classified based upon the index.

In the winter season December-January-February (DJF) of 1986–1987, the Northern Hemisphere flow pattern departed only slightly from that expected for an El Niño event: there was a strong West Coast ridge of high pressure (Fig. 3) and an associated split jet stream over the West Coast. During this winter, the southern branch of the jet stream, which often brings wet weather to southern California, was not very active. Furthermore, the northern branch was displaced well to the north so that the West Coast ridge of high pressure was effective in suppressing the normal passage of rain-producing low-pressure systems and associated cold fronts into the Western States and subsequently into the northern Plains States, leading to the drought development shown in the second panel of Fig. 1. Many of these storms were diverted northward into the Gulf of Alaska and never entered North America (*13*).

Conditions similar to those depicted for DJF 1986–1987 also occurred in several other months in 1987, and in particular, from September 1987 to March 1988, as shown for instance, by departure from normal (anomaly) pressure fields for September-October-November 1987 and DJF 1987–1988 (*9*). Thus throughout this period the atmospheric anomalies were consistent with the persistent oceanic anomalies depicted in Fig. 2.

The Summer Drought of 1988

During the spring of 1988 the situation changed significantly. From April to June 1988 the drought in the North Central United States and parts of the Northeast developed rapidly and dry conditions were exacerbated elsewhere, especially in the northern Plains (contrast the middle and bottom panels of Fig. 1). Many districts in Wisconsin, Illinois, Indiana, and Ohio, and some areas of Iowa, Missouri, and Michigan experienced the driest April-May-June since 1895 (*14*). The extent of the rainfall shortfall is revealed by precipitation percentiles for North America for April to June 1988 (Fig. 4).

By 23 July 1988, 43% of the area of the contiguous United States was in the severe or extreme drought category (*6*), a value that has been exceeded in only four previous years: 1934, 1936, 1954, and 1956. Clearly, the development and intensification of the drought during April to June 1988 was extremely unusual. But as shown in Fig. 1, the national drought was a combination of two or more regional droughts, each beginning at different times and involving different factors.

The atmospheric circulation over the United States was quite anomalous during April, May, and June 1988. During all 3 months strong anticyclonic conditions (high pressures or geopotential heights) were maintained in the upper atmosphere (for instance at 300 mb near the jet stream level) over the North Central United States (Fig. 5), pressures were low just off the West Coast and in the Gulf of Alaska, and pressures were high near 30°N just north of Hawaii. This pattern of highs and lows represented a wavetrain (double line in Fig. 5). The stationary wavetrain extended to a low center over the southeast United States, but this low was less persistent in location and was centered farther north in June. Elsewhere in the hemisphere, the pattern varied considerably from month to month. The positive geopotential height anomaly over the United States was most intense in June (+220 m at 300 mb, versus +70 m in April and +120 m in May). The 300 mb pattern for just May and June is similar to the April to June pattern (Fig. 5), except that all centers were more intense in May and June (+160 m over

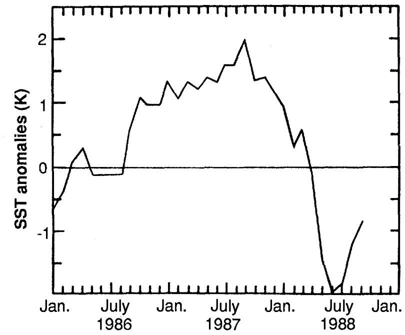

Fig. 2. Sequence of area-averaged SST anomalies for the "Niño 3" region from 5°N to 5°S, 90° to 150°W in the equatorial eastern Pacific Ocean from January 1986 through September 1988. The homogeneity of SST anomalies in this region can be judged from Fig. 6.

North America). Because the pattern was most distinctive in May and June, we focus on that period in the next sections.

These circulation anomalies (Fig. 5) would be expected to produce the observed precipitation anomalies (Fig. 4). The main deficit in rainfall occurred downstream from the ridge of high pressure over the eastern half of the nation. Although dry conditions continued also in the northern United States, the anomalous southerly air flow on the western side of the North American high (Fig. 5) helped bring moisture to the southwest, enhancing the effects of the early summer monsoon there. Thus, the main factor in the North American drought is the large-scale atmospheric circulation that extended well beyond North America and covered nearly half of the Northern Hemisphere.

Because a stationary wavetrain, such as that shown in Fig. 5, can be stimulated by a source in the tropical Pacific in winter *(12, 15)*, we investigated whether a linkage between these large-scale atmospheric anomalies and conditions in the tropical Pacific Ocean could have occurred during the summer of 1988.

Events in the Pacific Ocean

Following the demise of the El Niño in the Pacific in January 1988, SSTs continued to decrease and by May were 1.4 K below normal over a broad area near the equator (Fig. 2) and 3 K below normal locally. In contrast, average May to June SSTs (Fig. 6) were slightly elevated to the north, from 10° to 20°N, 110° to 150°W. As a result of these patterns, the strong convection in the intertropical convergence zone (ITCZ) shifted northward, as revealed by anomalies in outgoing long-wave radiation (OLR) measured by satellite (Fig. 7). The OLR data serve as an index of the amount of convection in the tropics, with negative anomalies indicating enhanced convective precipitation. The intensity of the ITCZ was close to normal, but its northward displacement resulted in a dipole in the OLR anomalies exceeding 15 W/m^2. Linear regressions of OLR data with rainfall rates over 2.5° latitude-longitude areas *(16)* indicate that a -20 W/m^2 anomaly in OLR is equivalent to a rainfall anomaly of ~4 mm/day or an anomalous latent heating rate of ~2.5 K per day if the heating occurs in a 400-mb layer. These numbers are subject to considerable uncertainty, but they provide a rough estimate of the anomalous heating rates that accompanied the ITCZ shift during April to June 1988.

Atmospheric Modeling

We have tested whether the stationary wavetrain shown in Fig. 5 could have been forced by the tropical heating anomalies (Fig. 7) with a global, primitive-equation, baroclinic, five-layer version of a stationary planetary wave model *(17)* that was linearized about climatological June conditions *(18)*. We carried out experiments in which idealized heating anomalies were used to represent the anomalous atmospheric forcing of the tropical eastern Pacific that is implicit in the OLR field (Fig. 7) *(19)*; more complete experiments will be possible when additional data are available on the forcing.

In the model, the resulting forced anomaly in the 300-mb geopotential height field (Fig. 8), reveals a wavetrain emanating from the tropical Pacific with the first three centers located close to those observed (Fig. 5), and, in particular, strong anticyclonic conditions over North America. The magnitude of the center of the North American high is just over 50 m, somewhat weaker than that observed. Heat sources in other parts of the domain, as well as many physical processes, some of which are discussed below, were not included in this calculation; therefore, it is not comprehensive. However, the agreement between the modeled and observed anomalies suggests that the mechanisms represented in the model could have been important in the real world.

Further calculations with the linear model suggest that some factors are of particular importance in producing the wavetrain (Fig. 8) across North America. The model response to only the vertical mean cooling in the equatorial region is shown in Fig. 9A (note that the contour interval is half of that in Fig. 8). In terms of amplitude, equatorial cooling does not make a large contribution to the

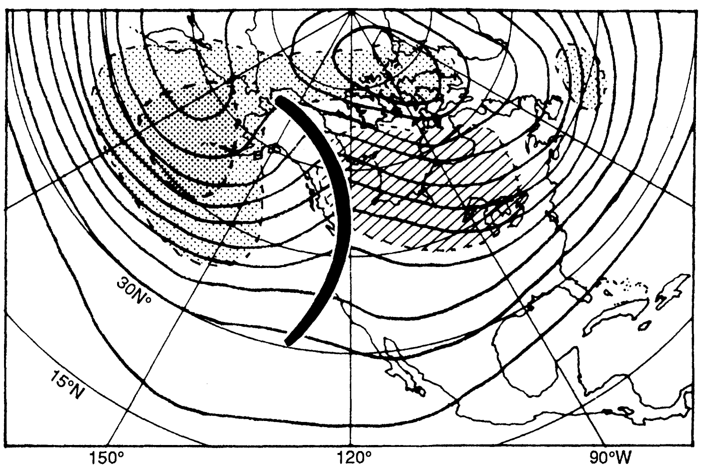

Fig. 3. Geopotential heights at 500 mb for DJF 1987. Shown are the total field with contours every 60 m (which indicate the mean flow), and departures from normal with hatched areas more than 50 m above normal and stippled regions more than 50 and 100 m (dense stipple) below normal. The heavy black line marks the ridge of high pressure.

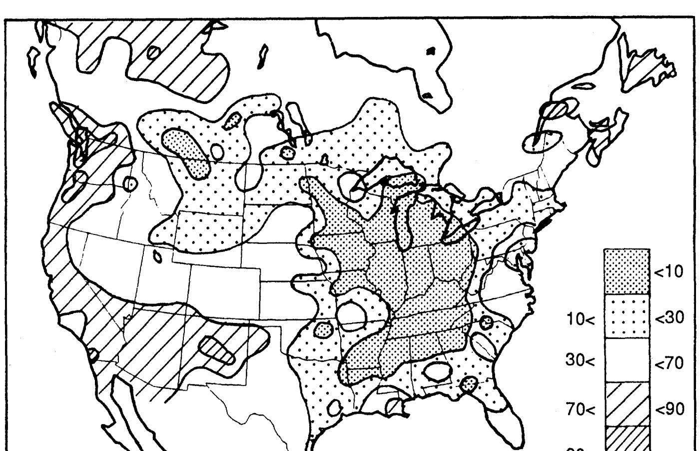

Fig. 4. Precipitation percentiles for North America for April-May-June 1988.

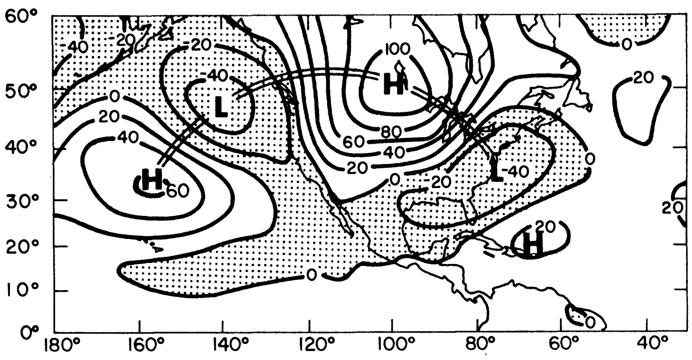

Fig. 5. Average geopotential height anomalies at 300 mb for April-May-June 1988. Contours are every 20 m and negative values are stippled. The high (H) and low (L) centers that formed the wavetrain are linked by the thin double line.

anomalous flow over North America. Rather, the wavetrain is primarily forced by the heating anomaly. But the structure of the response to cooling is somewhat similar; thus it tends to reinforce the effects of the heating anomaly.

Because most earlier modeling of this sort has been done with a zonally symmetric mean flow basic state (*20*), we performed a third experiment in which the model was linearized about the zonal mean component of the June flow, but with the same forcing as in our first experiments (Fig. 8). The results (Fig. 9B) indicate that climatological waves are important in producing the midlatitude pattern, as the magnitude of the midlatitude response is reduced to 20% of the value in Fig. 8. Furthermore, a comparison of Fig. 8 with Fig. 9B shows that zonal asymmetries in the climatological flow strongly influence the wavetrain structure (*21*).

Causes of the Drought

The evidence suggests that persistent global-scale anomalies in the atmospheric circulation set the stage for the drought in the United States. Large-scale circulation anomalies have also been associated with earlier U.S. droughts (*4, 5*). In summer droughts, there has always been upper-level anticyclonic conditions over the United States, usually associated in a wavelike pattern with a deeper than normal upper-level trough along the west coast of North America and another anticyclonic region over the central North Pacific. However, this teleconnection pattern has usually been oriented more east-west than that observed in 1988 (Fig. 5). Therefore, conclusions concerning the 1988 event may not be generally applicable to other United States droughts. The 1988 summer teleconnections were also markedly different from wintertime teleconnection patterns such as the Pacific–North American (PNA) pattern (*10*).

The configuration of SST anomalies in the tropical Pacific in 1988 resulted in anomalous atmospheric heating and cooling in the vicinity of the ITCZ, and the results of our preliminary modeling support our hypothesis that this pattern forced a wavetrain of high and low pressure anomalies across North America much like that observed. However, several other factors may have contributed to the circulation pattern across North America, including other anomalies in the heating field, such as the enhanced convective activity in the western Pacific south of Japan (*22*) indicated by the OLR data (Fig. 7). The presence of negative SST anomalies in the North Pacific Ocean (Fig. 6), which has been linked to previous droughts (*5*), could also have had an effect. In addition, the OLR anomalies over North America (Fig. 7) were distributed as a wavelike sequence of heating and cooling anomalies that could have reinforced the atmospheric flow anomalies locally.

In general in summer, once anticyclonic conditions prevail over the United States, other more local factors probably help maintain droughts and produce heat waves. In particular, land-surface processes involving the absence of soil moisture probably have a significant effect (*23*). Normally, heating from the sun is partitioned into evapotranspiration and sensible heating of the surface and atmosphere. But in drought conditions, evaporation and plant transpiration are greatly reduced so that nearly all heating is manifested as temperature increases. Moreover, the absence of moisture conspires against widespread precipitation. Heat waves result and a drought becomes, at least in part, self-perpetuating. Any greenhouse gas effects may have slightly exacerbated these overall conditions during the 1988 drought, but they almost certainly were not a fundamental cause.

We have shown that tropical teleconnections can occur in summer. This possibility has been in doubt because Rossby waves whose source is embedded in the tropical easterlies are trapped. However, divergent winds in the upper troposphere that result from anomalous tropical heating can extend outside of the tropics and thereby more effectively force atmospheric Rossby waves in mid-latitudes (*24*). Our calculations indicate that, in summer, the influence of tropical heating on North America depends greatly on the presence of the climatological waves in the Northern Hemisphere. This influence can be felt in several ways. In June, the zonal mean easterlies extend from south of the equator to ~20°N at 300 mb, but the easterlies are most extensive in the Asian sector of the Northern Hemisphere. As such, they prevent equatorial waves from radiating into midlatitudes (*12*). But in the Pacific, the easterlies are

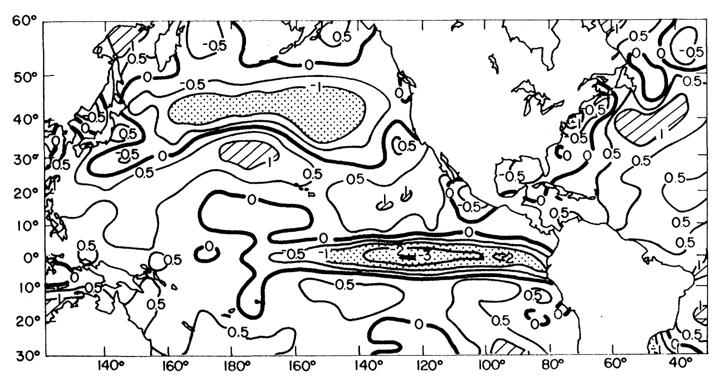

Fig. 6. Average May-June 1988 SST anomalies. The zero contour is the heavy line and contours are at ±0.5, ±1, ±2, and ±3 K. Values <−1 K are, stippled; values >1 K are hatched.

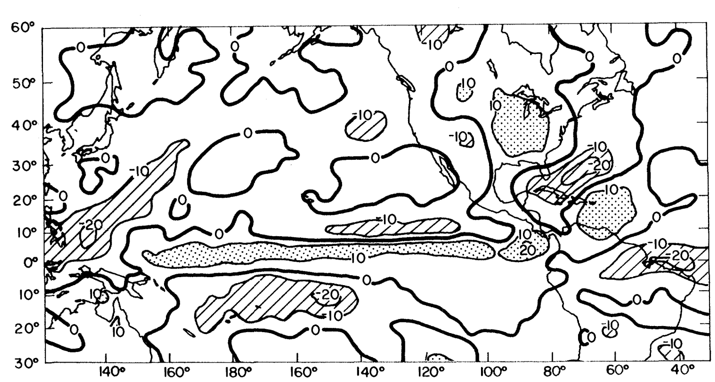

Fig. 7. Average May-June 1988 OLR anomalies. The zero contour is the heavy line and contours are every 10 W/m^2. Values >10 W/m^2 are stippled; values <−10 W/m^2 are hatched.

confined south of ~10°N, thus making tropical-extratropical teleconnections possible (*25*). The mean waves also act to refract perturbations emanating from the tropics (*25*) and wind shears associated with the mean waves can serve as local energy sources for the remotely stimulated waves (*26*).

The observed wavetrain (Fig. 5) varied somewhat from month to month, especially in the location of the downstream centers. In part, this variation was probably caused by transience in the atmosphere associated with weather changes generated by internal dynamical mechanisms. But evolution of the forcing in the tropical Pacific most likely also had an effect. The Rossby wave response is particularly sensitive to the latitude of the anomalous forcing, and

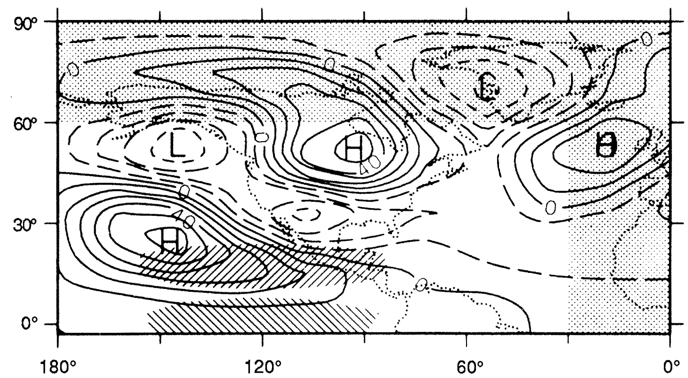

Fig. 8. Geopotential height anomalies at 300 mb resulting from the model simulation with the model linearized about June conditions and forced by heating in the northern hatched region and cooling in the southern hatched region in the tropical Pacific. The boundary of the hatched area indicates where the forcing is 20% of the maximum value. The stippled area denotes the region not shown in Fig. 5. The contour interval is 10 m and negative contours are dashed.

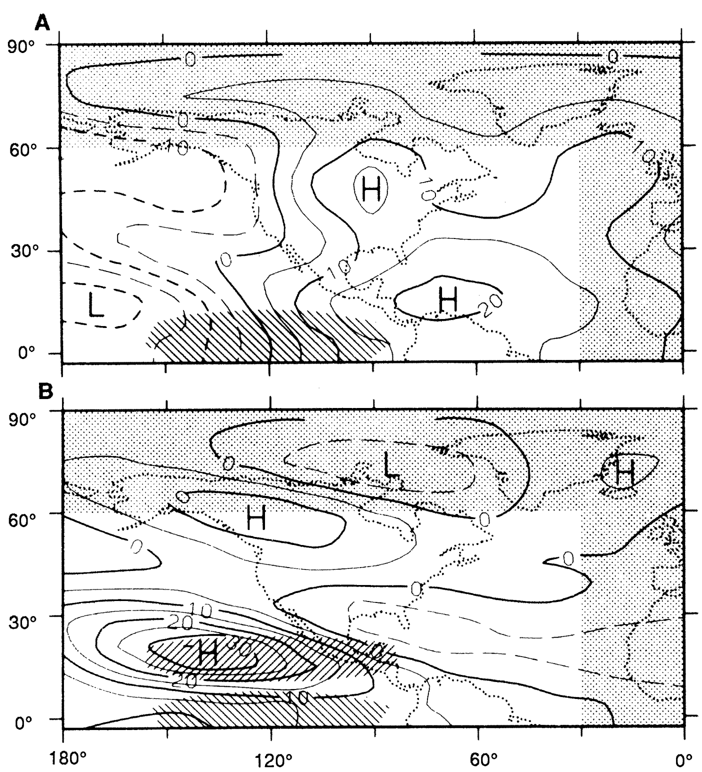

Fig. 9. Geopotential height anomalies at 300 mb resulting from the model simulation but with (**A**) only the cooling region present, and (**B**) with only zonal mean June conditions as the basic state. The contour interval is 5 m and negative contours are dashed.

interference from perturbations forced from other regions can affect the atmospheric flow over North America (*11, 12*).

The atmospheric circulation anomalies in 1988 in the northern hemisphere were associated with the changes in SSTs in the tropics. Circulation anomalies were also extreme, persistent, and extensive in the Southern Hemisphere (*9*) and may have been forced by the enhanced tropical connective activity there, as indicated by the OLR anomaly (Fig. 7). The convection occurs as part of the South Pacific convergence zone above warmer than normal water to the south of the cold equatorial tongue (Fig. 6). Thus it is possible that changes in tropical SSTs during 1988 may have evoked global atmospheric responses.

The mechanisms that we have discussed are natural phenomena that affect the entire climate system (not just the atmosphere). In particular, coupled interactions between the atmosphere and ocean play an important role and are strongest in the tropics (*27*). The atmosphere, through changes in trade winds, is responsible for changes in ocean currents and setting up the SST anomalies, which then, in turn, feed back and change the atmospheric circulation with teleconnections into higher latitudes. There are many possible variations on this theme, and previous droughts in the United States need not have originated in the same way. Further understanding of these processes and improved models of both the atmosphere and ocean raise the possibility that the results of these interactions may lead to more reliable predictions of short-term climatic conditions a season or two ahead.

REFERENCES AND NOTES

1. V. Ramanathan, *Science* **240**, 293 (1988).
2. G. A Meehl and W. M. Washington, *J. Atmos. Sci.* **45**, 1476 (1988); W. M. Kellogg and Z.-C. Zhao, *J. Climate* **1**, 348 (1988); S. Manabe and R. J. Stouffer, *Clim. Change* **3**, 347 (1981); S. Manabe and R. T. Wetherald, *Science* **232**, 626 (1986); *J. Atmos. Sci.* **44**, 1211 (1987).
3. H. F. Diaz, *J. Clim. Appl. Meteorol.* **22**, 3 (1983).
4. F.-C. Chang and J. M. Wallace, *Mon. Weather Rev.* **115**, 1253 (1987); W. H. Klein, *ibid.* **80**, 99 (1952).
5. J. Namias, *ibid.* **110**, 824 (1982).
6. *Weekly Weather Crop Bull. 75* [U.S. Department of Commerce, U.S. Department of Agriculture (USDA), Washington, DC, 2 August 1988].
7. The Palmer drought severity index is estimated by the National Oceanic and Atmospheric Administration (NOAA) USDA Joint Agricultural Weather Facility and published in the *Weekly Weather Crop Bull.* It provides a measure of prolonged abnormal dryness or wetness and reflects long-term moisture runoff, recharge, deep percolation, and evapotranspiration. It changes only slowly from week to week. Figure 1 is adapted from the published charts.
8. K. E. Trenberth, in *Contribution of Geophysics to Climate Change Studies*, A. Berger, R. Dickinson, J. Kidson, Eds. (American Geophysical Union, Washington, DC, in press).
9. *Climate Diagnostics Bull.*, published monthly by the Climate Analysis Center (NOAA, U.S. Department of Commerce, Washington, DC, 1987–1988).
10. H. van Loon and J. Rogers, *Mon. Weather Rev.* **109**, 1163 (1981); J. D. Horel and J. M. Wallace, *ibid.*, p. 813; E. M. Rasmusson and J. M. Wallace, *Science* **222**, 1195 (1983).
11. G. Branstator, *J. Atmos. Sci.* **42**, 2225 (1985).
12. B. J. Hoskins and D. J. Karoly, *ibid.* **38**, 1179 (1981).
13. *Mariners Weather Log* **31**, R. M. DeAngelis, Ed. (NOAA, U.S. Department of Commerce, Washington, DC, 1987).
14. According to preliminary estimates from NOAA, *Drought Advisory* **88, no. 4,** 13 July 1988.
15. J. D. Opsteegh and H. Van Den Dool, *J. Atmos. Sci.* **37**, 2109 (1980).
16. Heating rates from OLR were established by P. A. Arkin [thesis, University of Maryland (1983)].
17. G. Branstator, in preparation. This version of the model is an extension of a commonly used barotropic model (*11*) but has σ (terrain-following) coordinates with σ levels at 0.9, 0.7, 0.5, 0.3 and 0.1. It has horizontal variations represented by six zonal wavenumbers as well as the zonal mean, each of which is composed of 16 spherical harmonics. Dissipation is primarily represented by Newtonian and Rayleigh terms which have characteristic times of 5 days in the lowest layer and 20 days elsewhere. Results in Figs. 8 and 9 are for the σ = 0.3 level, which is close to 300 mb.
18. K. E. Trenberth and J. G. Olson, *Nat. Ctr. Atmos. Res. Tech. Note 300* **(1988)**.
19. The anomalous forcing is in the form of an elongated dipole with maximum values extending between 105° and 135°W and going to zero at 75° and 165°W. Maximum vertical mean heating is centered at 15°N and maximum vertical mean cooling is at 5°N, both decreasing to zero within ±5° latitude. At 15°N the vertical forcing profile consists of uniform heating in the model layers centered at

σ = 0.5and 0.3 with peak values of 2.5 K per day, and cooling in the top layer (σ = 0.1) at half this rate. This cooling represents anomalous radiative cooling at cloud top as measured by the OLR anomaly. The upper tropospheric heating in a 400-mb layer follows D. L. Hartmann, H. H. Hendon, R. A. Houze [*J. Atmos. Sci.* **41**, 113 (1984)]. At 5°N the sign of the vertical profile of forcing is reversed.
20. R. Mureau, J. D. Opsteegh, J. D. Winston, *Mon. Weather Rev.* **115**, 856 (1987).
21. Other preliminary experiments support the robustness of our results. When the climatological waves are retained, the structure of the response is rather insensitive to the exact longitude of the heating. Point sources at all locations at 15°N between 100° and 150°W, but not elsewhere, produce essentially the same midlatitude pattern, although with varying amplitude. Changes in the vertical heating profile in the model also alter the amplitude but not the pattern of the response.
22. K. Kurihara and T. Tsuyuki, *J. Meteorol. Soc. Jpn.* **65**, 237 (1987); T. Nitta, *ibid.*, p. 373.
23. W. D. Sellers, *Physical Climatology* (Univ. of Chicago Press, Chicago, 1965); J. Shukla and Y. Mintz, *Science* **215**, 1498 (1982); T.-C. Yeh, R. T. Wetherald, S. Manabe, *Mon. Weather Rev.* **112**, 474 (1984).
24. P. D. Sardeshmukh and B. J. Hoskins, *J. Atmos. Sci.* **45**, 1228 (1988).
25. G. Branstator, *J. Atmos. Sci.* **40**, 1689 (1983), P. A. Webster and J. Holton, *ibid.* **39**, 722 (1982).
26. A. Simmons, J. M. Wallace, G. Branstator, *J. Atmos. Sci.* **40**, 1363 (1983).
27. S. E. Zebiak and M. A. Cane, *Mon. Weather Rev.* **115**, 2262 (1987).
28. The National Center for Atmospheric Research is sponsored by the National Science Foundation.

Laser Femtochemistry

Ahmed H. Zewail

Femtochemistry is concerned with the very act of the molecular motion that brings about chemistry, chemical bond breaking, or bond formation on the femtosecond (10^{-15} second) time scale. With lasers it is now possible to record snapshots of chemical reactions with sub-angstrom resolution. This strobing of the transition-state region between reagents and products provides real time observations that are fundamental to understanding the dynamics of the chemical bond.

The molecular events that bring about chemistry, chemical bond breaking or bond formation, occur with awesome rapidity, often in less than 10^{-12} s. One of the fundamental problems in chemistry is to understand how these events, which occur in the region of the transition state between reagents and products, determine the entire course of the reaction, including the fate of the products. In the past the actual dynamics of this region could not be time-resolved, but chemists devised methodologies for describing reactivity. Different approaches (for example, thermodynamics, kinetics, and synthesis) have been used to systematize a large body of experimental data and obtain the energetics (ΔG, ΔH, and so forth), the rates [$k(T)$], and the mechanisms of the reactions, thus establishing the macroscopic picture.

Understanding the detailed dynamics of reactions on the molecular level required new microscopic methods (*1–3*), which were introduced some 30 years ago. Major advances have come from the application of molecular beam, chemiluminescence, and laser techniques (*4*). In the simplest molecular beam experiments, a beam of reagent molecules is directed towards co-reagent molecules (in the form of a target gas or another beam), and the reactive scattering that leads to product molecules is observed. The relative kinetic energy of the reagents can be changed by varying the velocity of one of the reagent molecules with respect to the other reagent involved in the "single collision." For laser–molecular beam experiments, a laser can be used to excite one of the reagent molecules and thus influence the reaction probability, or the laser can initiate a unimolecular process by depositing energy in a molecule. In this so-called "half-collision" unimolecular process, the fragmentation of the excited molecule, which can be represented as ABC into A and BC, is the dynamical process of interest.

The ingeniousness of this approach is in using the postcollision (or half-collision) attributes of the products (angular distributions, population and energy distributions, alignment, and so forth) to infer the dynamics of the reactive collision (or half-collision). During the last three decades many reactions have been studied and these methods, with the help of theory, have become the main source of information for deducing the nature of the potential energy surface (PES) of the reaction (*4*).

To directly observe the transition-state region between reagents and products, which is the fundamental feature of reaction dynamics, different methodology is needed. As mentioned above, these states are ultrashort-lived and experiments on a longer time scale provide data that are effectively time-integrated over the course of the collision or half-collision. Smith (*5*), in comparing different experimental approaches, noted that a great deal is known about the "before" and "after" stages of the reaction, but that it is difficult to observe the "during" phase. The problem is perhaps illustrated best by the quotation of Zare and Bernstein (*6*), which describes the choreography of these processes: "The study of chemical reaction kinetics can be likened to the task of making a motion picture of a reaction. The trouble thus far with achieving this goal seems to be the problem of too many would-be actors who strut upon the stage without proper cue and mumble their lines too rapidly to be understood—for chemical reactions occur with the ease of striking a match and at a speed so fast (on a subpicosecond time scale for the making of new bonds and breaking of old ones) as to be a severe challenge to the moviemaker who would like to record individual frames."

In recent years, great progress has been made by several groups (*7–13*) using absorption, emission, scattering, and ion spectroscopy to probe the relevant transition region. Without direct time resolution, they used these clever methods, reviewed recently by Polanyi (*7*), Kinsey (*8*), and Brooks and Curl (*9*), to obtain information on the dynamics in the transition-state region of some elementary reactions. Examples include the dissociation of methyl iodide (*8*)

The author is a professor of chemistry at the Arthur Amos Noyes Laboratory of Chemical Physics, California Institute of Technology, Pasadena, CA 91125.